Carcinogenesis vol.35 no.2 pp.461–468, 2014
doi:10.1093/carcin/bgt335
Advance Access publication October 8, 2013

CYLD controls c-MYC expression through the JNK-dependent signaling pathway in hepatocellular carcinoma

Rajeswara Rao Pannem, Christoph Dorn[1], Kristofer Ahlqvist, Anja K.Bosserhoff[2], Claus Hellerbrand[1] and Ramin Massoumi*

Department of Laboratory Medicine, Skåne University Hospital, Lund University, Malmö SE-20502, Sweden, [1]Department of Internal Medicine I, University Hospital of Regensburg, Regensburg 93053, Germany and [2]Institute of Pathology, University of Regensburg, Regensburg 93053, Germany

*To whom correspondence should be addressed. Tel: +46 40 331228; Fax: +46 40 337063;
Email: Ramin.Massoumi@med.lu.se

Posttranslational modification of different proteins *via* direct ubiquitin attachment is vital for mediating various cellular processes. Cylindromatosis (CYLD), a deubiquitination enzyme, is able to cleave the polyubiquitin chains from the substrate and to regulate different signaling pathways. Loss, or reduced expression, of CYLD is observed in different types of human cancer, such as hepatocellular carcinoma (HCC). However, the molecular mechanism by which CYLD affects cancerogenesis has to date not been unveiled. The aim of the present study was to examine how CYLD regulates cellular functions and signaling pathways during hepatocancerogenesis. We found that mice lacking CYLD were highly susceptible to chemically induced liver cancer. The mechanism behind proved to be an elevated proliferation rate of hepatocytes, owing to sustained c-Jun N-terminal kinase 1 (JNK1)-mediated signaling *via* ubiquitination of TNF receptor-associated factor 2 and expression of c-MYC. Overexpression of wild-type CYLD in HCC cell lines prevented cell proliferation, without affecting apoptosis, adhesion and migration. A combined immunohistochemical and tissue microarray analysis of 81 human HCC tissues revealed that CYLD expression is negatively correlated with expression of proliferation markers Ki-67 and c-MYC. To conclude, we found that downregulation of CYLD induces tumor cell proliferation, consequently contributing to the aggressive growth of HCC. Our findings suggest that CYLD holds potential to serve as a marker for HCC progression, and its link to c-MYC *via* JNK1 may provide the foundation for new therapeutic strategies for HCC patients.

Introduction

Hepatocellular carcinoma (HCC) is one of the leading causes of cancer-related death worldwide. HCC typically arises in patients with hepatitis (also viral) or cirrhosis in combination with accumulating genetic alterations, including mutation of tumor suppressor and/or proto-oncogenes (1–3). Since the prognosis remains poor for patients diagnosed at an advanced stage, there is a need for improved diagnosis and treatment.

Ubiquitination and deubiquitination are established mechanisms for cellular homeostasis; dysregulation occurring in this system alters the function of the cell. Generally, polyubiquitination of any substrate through Lys-48-linkage, targets the protein for proteasome-mediated degradation, whereas Lys-63-linked ubiquitin chains add new functional properties to the modified protein (4,5). Ubiquitination is reversible by action and activation of deubiquitination enzymes (6,7). We, and others, have demonstrated that the *cylindromatosis* (*CYLD*) gene product, which is a deubiquitination enzyme, functions as a tumor suppressor in different types of cancer, such as melanoma, basal cell carcinoma and colon and lung cancer (8–12). By removing ubiquitin chains from the different substrates, including the TNF receptor-associated factor 2/6 (TRAF2/6), the transforming growth factor β-activated kinase 1 and the B-cell lymphoma 3-encoded protein (Bcl-3), CYLD interferes with signaling pathways, such as nuclear factor kappa B (NF-κB) and c-Jun N-terminal kinase (JNK), thus regulating cell proliferation and cell survival (13–15). The involvement of CYLD is not restricted to removal of Lys-63 polyubiquitin chains from different substrates but has been shown to interfere with other signaling pathways as well, independent of its deubiquitin activity (16).

We have shown previously that the CYLD messenger RNA expression in HCC, *in situ* as well as in cell lines, is downregulated in comparison with non-neoplastic tissue samples or cells (17). Recent studies demonstrated that CYLD is an important regulator of hepatocyte homeostasis, by protecting cells from apoptosis, which further prevents the initiation phase of HCC development (18,19). Furthermore, overexpression of CYLD in HCC cell lines decreases NF-κB activation, augmenting the antitumorous effect of TRAIL (18), caused by a direct binding of CYLD to IkB kinase gamma subunit in TRAIL-mediated NF-κB signaling (20). Notably, CYLD expression alone in HCC cell lines had minor antitumor activity, whereas a combinational expression of CYLD and TRAIL initiated apoptosis in those cells (20). In another recent study, downregulation of CYLD resulted in an increased resistance to treatment with anticancer drugs, suggesting that CYLD expression plays a major role in overcoming therapy resistance in HCC (21,22). Notwithstanding these significant observations, the molecular mechanism by which CYLD affects hepatocancerogenesis has yet not been unveiled.

In the present study, we revealed that CYLD critically affects proliferation in HCC cells *in vitro*, and in an experimental HCC model in mice. We observed an inverse correlation between loss of CYLD expression and cell proliferation in human HCC tissues, and we found that CYLD, *via* JNK1, inhibits the c-MYC expression in HCC cells.

Abbreviations: Bcl-3, B-cell lymphoma 3-encoded protein; CYLD, cylindromatosis; DEN, diethylnitrosamine; HCC, hepatocellular carcinoma; JNK1, c-Jun N-terminal kinase 1; NF-κB, nuclear factor kappa B; TMA, tissue microarray; TRAF, TNF receptor-associated factor 2.

Materials and methods

Cells and cell culture

Primary murine hepatocytes were isolated, using a modified two-step ethyleneglycol-bis(aminoethylether)-tetraacetic acid/collagenase perfusion procedure, and cultured as described previously (23). The HCC cell lines HepG2 (ATCC HB-8065), PLC (ATCC CRL-8024), Huh7 (ATCC PTA-4583) and Hep3B (ATCC HB-8064) were cultured as described previously (24).

Animals, experimental in vivo models and ethical consideration

Generation of CYLD knockout (KO or *CYLD*$^{-/-}$) mice has been described previously (10). All mice were maintained in specific pathogen-free housing at the Clinical Research Centre in Malmö, and the animal experiments were performed according to national and international guidelines of the European Union. To induce hepatocarcinogenesis, male mice were injected intraperitoneally with 25 mg/kg of diethylnitrosamine (DEN) (Sigma–Aldrich, Stockholm, Sweden) at the age of 15 days and were subsequently observed for development of tumors. The cohort was killed at 12 months of age, in accordance with the protocol. For short-term studies of acute liver injury, 15 days old mice were injected intraperitoneally with DEN. The mice were subsequently killed at the indicated time points (3, 6, 12, 24, 48, 72 h after injection). JNK inhibition was accomplished by injection (intraperitoneally) of 30 µg/g body weight of the JNK-specific inhibitor SP600125 (Sigma–Aldrich) 1 h prior to DEN injection. Control mice received only the solvent dimethyl sulfoxide.

HCC tissue microarrays and immunohistochemical analyses

Tissue microarrays (TMA) were constructed (as described in refs 24,25), consisting of 85 formalin-fixed, paraffin-embedded human HCC tissues, and corresponding non-neoplastic liver tissue of the same patient (in 80 cases). Clinicopathological patient characteristics are summarized in Supplementary Table 1, available at *Carcinogenesis* Online. Immunohistochemical staining of 5 µm sections of the TMA blocks was performed, using a CYLD antibody (rabbit polyclonal, 1:100, #SAB4200060 from Sigma–Aldrich) or a c-MYC antibody (rabbit polyclonal, 1:50, from Abcam), utilizing an

indirect immunoperoxidase protocol in accordance with the LSAB2-kit (DAKO, Hamburg, Germany). The primary antibody was omitted for negative control; the immunoglobulin G isotype control antibodies did not produce any detectable staining. For the TMA evaluation, any detectable cytoplasmic staining was defined as the tissue sample being CYLD positive, and detectable nuclear staining was defined as the tissue sample being c-MYC positive. In contrast, samples designated as CYLD negative or c-MYC negative did not reveal any immunohistochemical staining. MiB-1 was analyzed by applying an anti-Ki-67 antibody (rabbit monoclonal, clone MiB-1, 1:10, final concentration of 5 g/ml; DAKO). Antibody binding was visualized by using an AEC solution (LSAB2-Kit; DAKO). Finally, the tissues were counterstained with hemalaun. Furthermore, immunohistochemical analyses of murine liver sections were performed, using rabbit polyclonal CYLD (1:600), rabbit polyclonal Bcl-3 (C-14), mouse monoclonal phospho-JNK1 (G-7) and polyclonal p65 (F-6) antibodies from Santa Cruz Biotechnology.

RNA isolation and real-time quantitative PCR

Total RNA was isolated from liver tissue and cells, using a nucleospin RNA II kit (Macherey-Nagel) in accordance with the manufacturer's instructions. Reverse transcription of total RNA (1.5 µg) into first strand complementary DNA was performed by means of an AffinityScript™ QPCR cDNA synthesis kit (Stratagene) for quantitative PCR, using oligo (deoxythymidine) primers. Quantitative PCR was performed using SYBR® Green QPCR master mix (Stratagene), and messenger RNA expression analyses were performed using QuantiTect Primer Assays, in accordance with the manufacturer's instructions (Qiagen, Hilden, Germany). Genes and primer sequences were: hCYLD, forward: 5′-TGC CTT CCA ACT CTC GTC TTG-3′ and reverse: 5′-AAT CCG CTC TTC CCA GTA GG-3′; hBeta actin, forward: 5′-CTA CGT CGC CCT GGA CTT CGA GC-3′ and reverse: 5′-GAT GGA GCC GCC GAT CCA CAC GG-3′; mCYLD, forward: 5′-ACA ACA TGG ATG CCA GGT TG-3′ and reverse: 5′-CCG CTA ATA AAG GTC CTC TG-3′; mGAPDH, forward: 5′-TCG TGG ATC TGA CGT GCC GCC-3′ and reverse: 5′-CAC CAC CCT GTT GCT GTA GCC-3′.

Statistical analyses

Statistical analyses were performed, using SPSS 15.0 (SPSS, Chicago, IL) and GraphPad Prism Software (GraphPad Software). Results are expressed as means ± SD or as percentages. Groups were compared by means of a paired *t*-test. Fisher's exact test was used to study the statistical association between clinicopathological and immunohistochemical variables. Significance was accepted at the level $P < 0.05$ (*). Further details of our methods can be found in supplementary methods.

Results

CYLD$^{-/-}$ *mice are highly sensitive to liver tumor development*

Mice lacking the *CYLD* gene have no obvious phenotype and have a normal life span (10). Immunohistochemical analyses showed that CYLD was ubiquitously expressed in human and murine liver tissues (Supplementary Figure 1, available at *Carcinogenesis* Online). Up to the age of 1 year, the liver of CYLD-deficient mice displayed regular cell morphology and cellular integrity, and they did not develop spontaneous liver tumors.

After a latency period of 12 months, we observed HCC development in both wild-type and CYLD knockout mice that at the age of 15 days had been exposed to the chemical carcinogen DEN (Figure 1A). Liver weight, tumor numbers, tumor size and maximal tumor size were significantly increased in *CYLD*$^{-/-}$ mice compared with control mice (Figure 1B–E). Furthermore, trabecular sinusoidal structures, a pathological alteration of liver plates frequently occurring in human HCC, which is related to the initiation stage of metastasis and invasion (26), were more prominent in tumor tissue of *CYLD*$^{-/-}$ mice than in control mice (Figure 1F).

CYLD-deficient tumors exhibit increased cell proliferation

The examination of the mechanism behind cell proliferation and cell apoptosis in HCC revealed that Ki-67 (Figure 2A) and cyclin D1 expressions (Figure 2B) were significantly increased in *CYLD*$^{-/-}$ tumors, as was the percentage of proliferating cell nuclear antigen-positive cells in the surrounding non-tumoral liver tissue (Figure 2C).

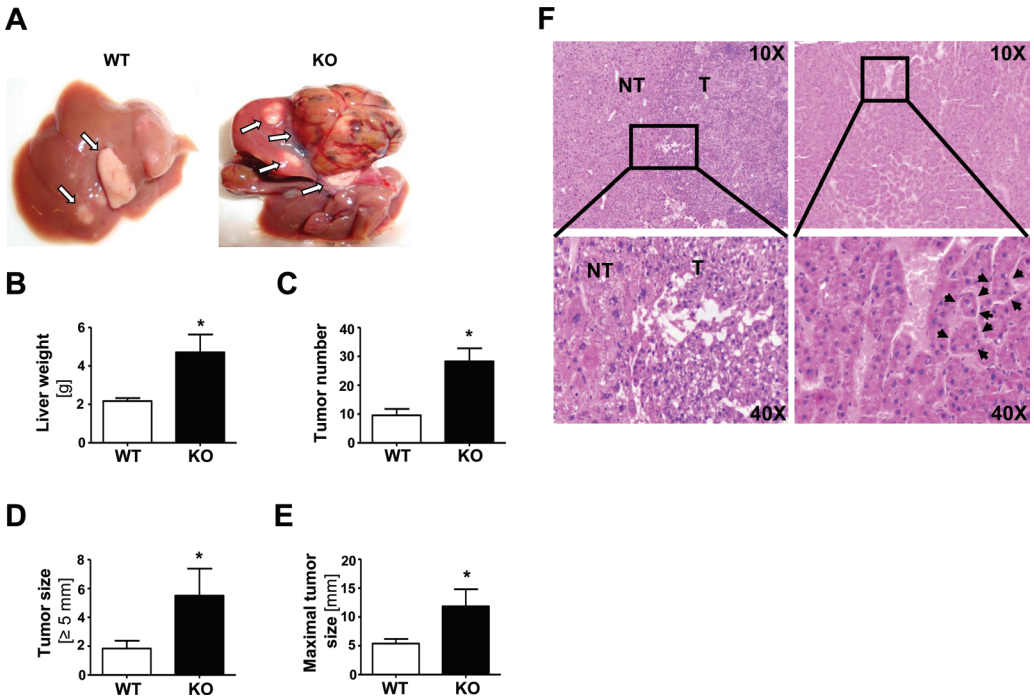

Fig. 1. Loss of CYLD potentiates DEN-induced liver tumor development in mice. (**A**) Mice were injected intraperitoneally with 25 mg/kg of DEN at 15 days of age, and livers of wild-type ($n = 16$) and CYLD-deficient mice [knockout (KO)] ($n = 16$) were isolated after a latency period of 12 months. (**B**) Mean total liver weight of wild-type ($n = 16$) and CYLD-deficient mice ($n = 16$). Results are means ± SD; *$P < 0.05$ denotes significant differences between the groups. (**C**) Number of tumors in wild-type ($n = 16$) and CYLD-deficient mice ($n = 16$). Results are means ± SD; *$P < 0.05$ denotes significant differences between the groups. (**D**) Size of the tumors (≥5 mm) in wild-type ($n = 16$) and CYLD-deficient mice ($n = 16$) after treatment *in situ* with DEN. Results are means ± SD; *$P < 0.05$ denotes significant differences between the groups. (**E**) Maximal tumor size in 12 months old wild-type ($n = 16$) and CYLD-deficient mice ($n = 16$). Results are means ± SD; *$P < 0.05$ denotes significant differences between the groups. (**F**) Hematoxylin and eosin staining of tumors isolated from wild-type and CYLD-deficient mice. Non-tumor (NT) and tumor (T) tissues of liver sections from wild-type mice are indicated in ×10 and ×40 magnifications. CYLD KO tumor tissue displays trabecular sinusoidal structures, which is absent in control tumor tissue (×40).

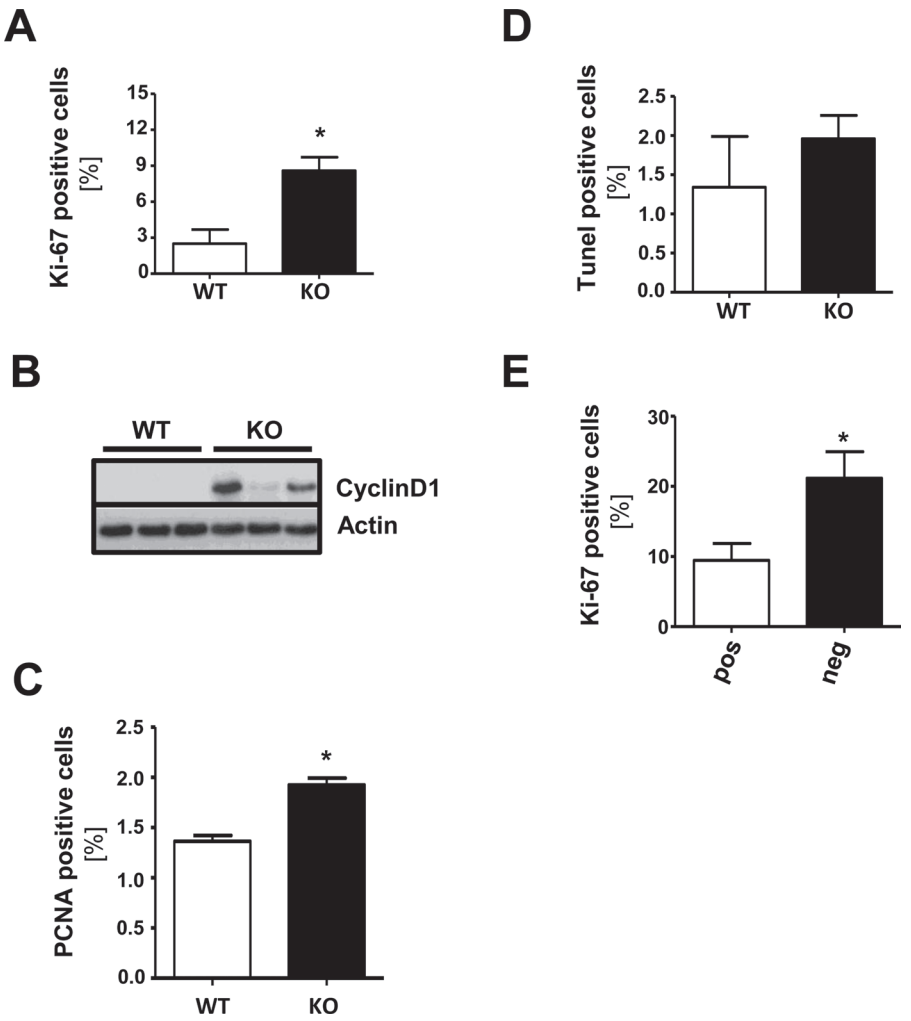

Fig. 2. Absence of CYLD is associated with increased cell proliferation in HCC. (**A**) Analysis of Ki-67-positive cells in tumors of wild-type and CYLD-deficient mice treated with DEN, 15 days after treatment and after a latency period of 12 months. Results are means ± SD; *$P < 0.05$ denotes significant differences between the groups. (**B**) The levels of cyclin D1 in three different tumors from 12 months old wild-type and CYLD-deficient mice, 1 year after DEN treatment. (**C**) Analysis of proliferating cell nuclear antigen (PCNA)-positive cells in non-tumorous liver tissue of 12 months old wild-type and CYLD-deficient mice, 1 year after DEN treatment. Results are means ± SD; *$P < 0.05$ denotes significant differences between the groups. (**D**) A terminal deoxynucleotidyl transferase-mediated dUTP nick end labeling (TUNEL) assay analysis of apoptotic cells in liver tumors of wild-type and CYLD-deficient mice, 15 days after treatment with DEN, and after a latency period of 12 months. (**E**) Proliferation rate (analyzed by immunohistochemical staining, using anti-Ki-67 antibodies) in HCC tissues showing positive or negative immunoreactivity to CYLD, applying TMA technology.

In addition, this effect was tissue specific, since the levels of cyclin D1 did not differ in other non-tumoral tissues, such as brain and lung, between the experimental groups (Supplementary Figure 2, available at *Carcinogenesis* Online). Furthermore, we did not detect any differences in the number of apoptotic cells between tumors isolated from wild-type and tumors from *CYLD*$^{-/-}$ mice (Figure 2D). These results were confirmed by using TMA technology (24,25) on a series of 81 HCC patients (Supplementary Table 1, available at *Carcinogenesis* Online), which revealed the CYLD expression to be negatively correlated with a high MiB-1 index (Supplementary Table 2, available at *Carcinogenesis* Online, Figure 2E). CYLD protein expression was found in all ($n = 75$) non-cancerous tissue samples; in 43.2% (35/81) of the HCC, no CYLD immunosignal was detectable. Representative immunohistochemical stainings of CYLD-positive and CYLD-negative tumor tissues are presented in Supplementary Figure 3, available at *Carcinogenesis* Online.

CYLD-deficient tumors exhibit increased JNK1 activation

The western blot analysis of liver tumors isolated from *CYLD*$^{-/-}$ and *CYLD*$^{+/+}$ mice revealed that tumors isolated from CYLD-deficient animals exhibited high levels of phospho-JNK1 (Figure 3A) under non-induced conditions, without affecting the total level of JNK1 (Figure 3B). Furthermore, tumors isolated from CYLD-deficient animals showed high levels of c-MYC and ubiquitinated TRAF2, compared with wild-type tumors (Figure 3C and D). No difference in the activation of extracellular signal-regulated kinase or Akt/protein kinase B was observed between wild-type tumors and CYLD-deficient tumors (Figure 3E).

Loss of CYLD promotes TRAF2-mediated JNK1 activation and proliferation in the acute phase of liver injury

In exploring the foundation for the increased susceptibility of *CYLD*$^{-/-}$ mice to chemically induced carcinogenesis, we observed that after 72 h, DEN treatment of liver tissue had significantly increased the number of proliferating cells in *CYLD*$^{-/-}$ mice (Figure 4A). Moreover, 72 h after treatment with DEN, the cyclin D1 expression was elevated in liver tissue isolated from *CYLD*$^{-/-}$ but not in *CYLD*$^{+/+}$ mice (Supplementary Figure 4, available at *Carcinogenesis* Online). The levels of p53 (Supplementary Figure 5, available at *Carcinogenesis* Online) or serum levels of aspartate aminotransferase (Supplementary Figure 6, available at *Carcinogenesis* Online) did not differ significantly between the experimental groups. DEN treatment (72 h) of

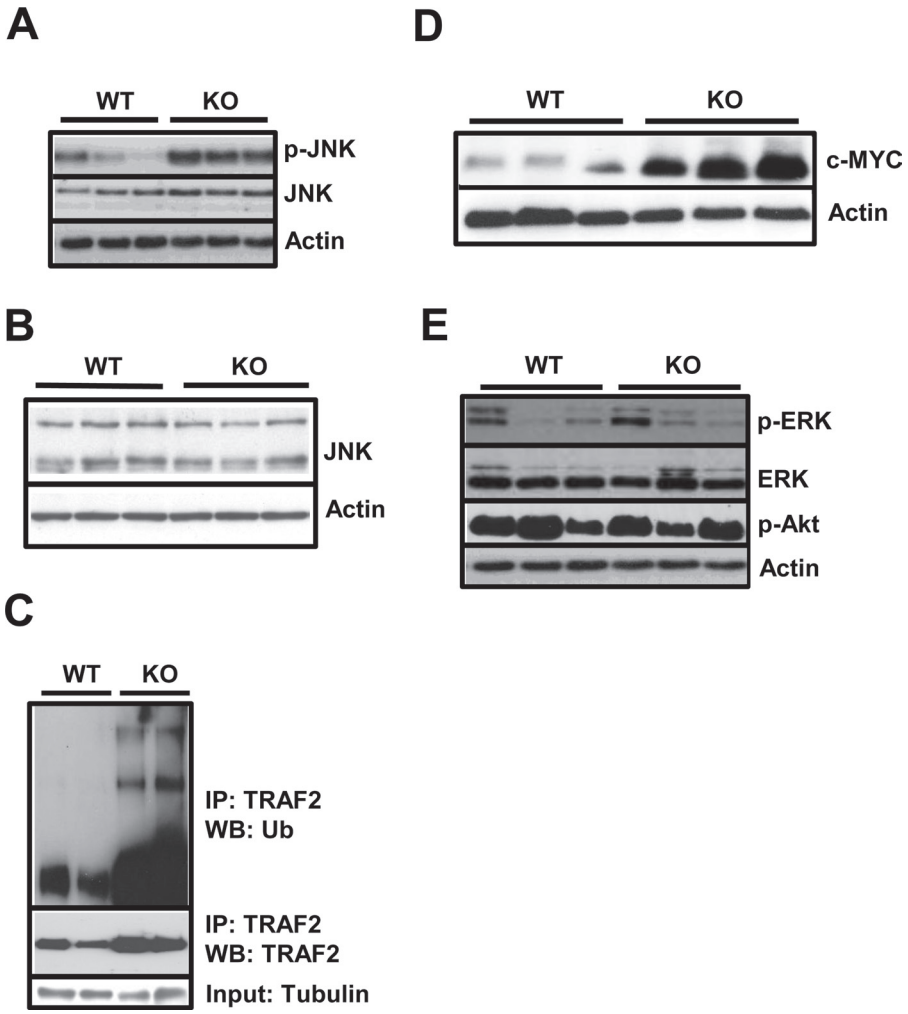

Fig. 3. Elevated activation of JNK1 in tumors isolated from CYLD-deficient mice. (**A**) The levels of phospho-JNK1 (p-JNK1) and total JNK1 in three different tumors from 12 months old DEN-treated wild-type and CYLD-deficient mice. (**B**) The levels of total JNK1 and actin in livers of adult (12 months) wild-type ($n = 3$) and CYLD-deficient mice ($n = 3$). (**C**) TRAF2 ubiquitination in two different tumors, isolated from 12 months old DEN-treated wild-type and CYLD-deficient mice. (**D**) The levels of c-MYC and actin in three different tumors from 12 months old DEN-treated wild-type and CYLD-deficient mice. (**E**) The levels of phospho-extracellular signal-regulated kinase (p-ERK), total ERK, phospho-Akt (p-Akt) and actin in three different tumors from 12 months old DEN-treated wild-type and CYLD-deficient mice.

liver sections isolated from $CYLD^{-/-}$ mice significantly increased the number of cells displaying nuclear staining of phospho-JNK1, but not of Bcl-3 or p65, in contrast to $CYLD^{+/+}$ mice (Figure 4B and Supplementary Figure 7, available at *Carcinogenesis* Online). Furthermore, DEN treatment *in vitro* resulted in an increase in JNK1 activation in hepatic tissue from $CYLD^{-/-}$ mice (Figure 4C) as well as in primary hepatocytes of $CYLD^{-/-}$ mice (Figure 4D), as compared with $CYLD^{+/+}$ hepatocytes. DEN exposure promoted upregulation of TRAF2 ubiquitination in $CYLD^{-/-}$ but not in $CYLD^{+/+}$ liver tissue (Figure 4E), and did not change the total level of TRAF2 (Supplementary Figure 8, available at *Carcinogenesis* Online). A significant increase in the levels of c-MYC (another downstream target protein responsible for JNK1-mediated proliferation of HCC) upon 48 h of DEN treatment was observed in $CYLD^{-/-}$ but not in $CYLD^{+/+}$ mice (Figure 4F). However, under non-induced condition, the levels of c-MYC was low and did not differ between $CYLD^{+/+}$ and $CYLD^{-/-}$ mice (Figure 4G).

CYLD expression in HCC cells reduces JNK1-mediated signaling and cell proliferation

The assessment of four different human HCC cell lines, analyzing whether the expression of CYLD is important for inhibition of JNK1-mediated cancer cell proliferation, revealed a reduced CYLD expression in all HCC cell lines in comparison with primary hepatocytes (Figure 5A; ref. 17). The expression of CYLD was inversely correlated with the proliferation capacity of the different HCC cell lines (Figure 5B). Overexpression of CYLD in HepG2, PLC and Huh7 cells reduced their proliferation rate (Figure 5C and Supplementary Figure 9A, available at *Carcinogenesis* Online). However, no differences were observed in the number of apoptotic cells, cell adhesion or migration in cells transfected with full-length CYLD in comparison with MOCK-transfected cells (Supplementary Figure 10, available at *Carcinogenesis* Online). Furthermore, overexpression of full-length CYLD reduced the levels of c-MYC, cyclin D1 and JNK1 phosphorylation (Figure 5D and Supplementary Figure 9B, available at *Carcinogenesis* Online), and also reduced TRAF2 ubiquitination (Figure 5E and Supplementary Figure 9C, available at *Carcinogenesis* Online) and transcriptional activity of AP-1 (Figure 5F and Supplementary Figure 9D, available at *Carcinogenesis* Online). Since downregulation of c-MYC did not influence the activity of JNK, this suggests that in HepG2 cells JNK activation operates upstream of c-MYC expression (Figure 6A). As expected, downregulation of c-MYC in HepG2, PLC and Huh7 cells reduced proliferation (Figure 6B and Supplementary Figure 11A and B, available at *Carcinogenesis* Online) but not the number of apoptotic cells (Figure 6C), and overexpression of CYLD reduced the c-MYC

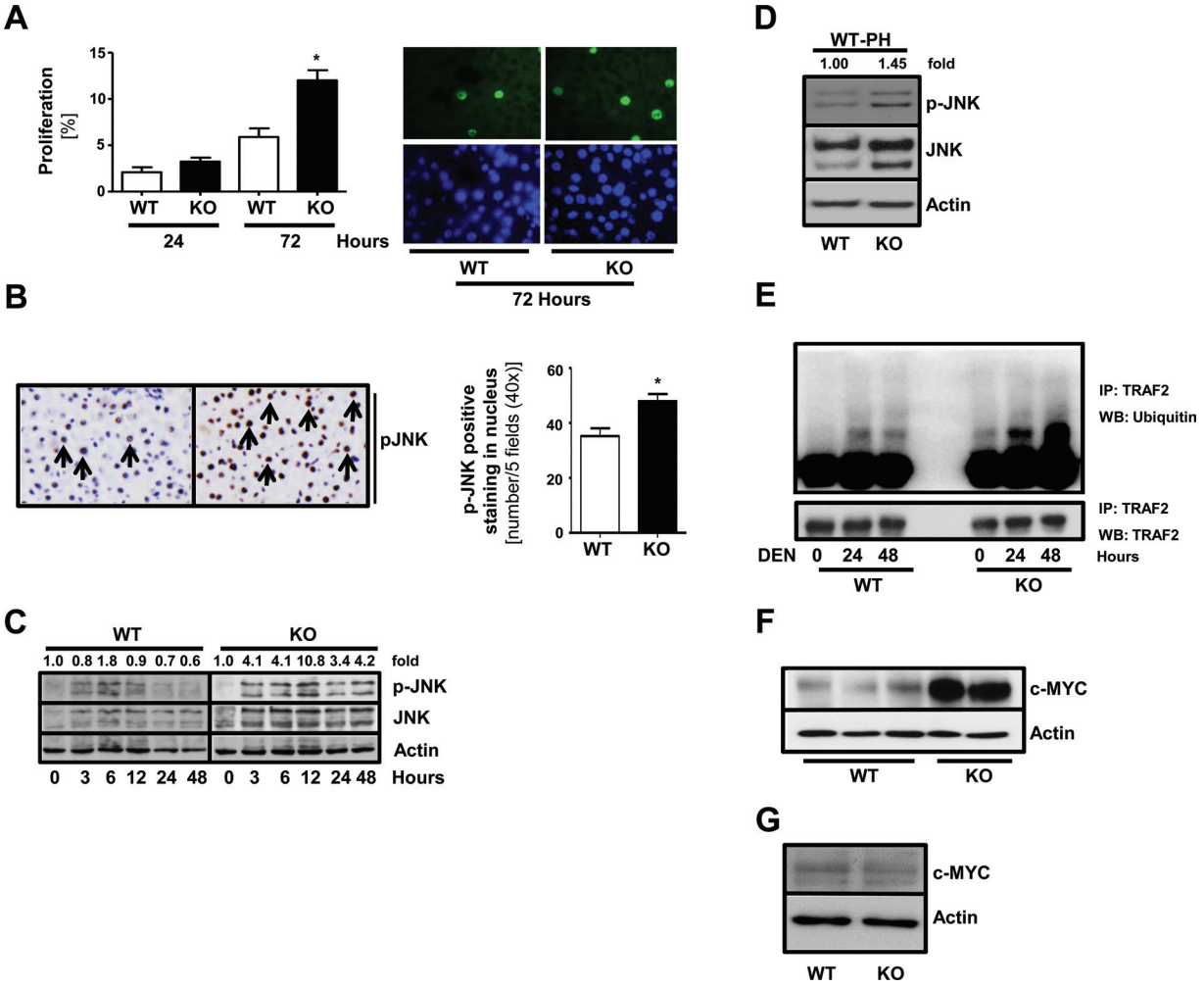

Fig. 4. JNK1 signaling mediates TRAF2 ubiquitination and cell proliferation in CYLD-deficient cells and tissues. (**A**) The presence of bromodeoxyuridine-positive cells in the liver of 15 days old wild-type ($n = 3$) and CYLD-deficient mice ($n = 3$) 24 and 72 h post-DEN treatment. Results are means ± SD of three separate experiments; $^*P < 0.05$ denotes significant differences between the groups. (**B**) Immunohistochemical analysis of phospho-JNK1 (p-JNK1) in livers of 15 days old wild-type ($n = 3$) and CYLD-deficient mice ($n = 3$) 72 h after DEN treatment. (**C**) The levels of p-JNK1 and total JNK1 in livers of 15 days old wild-type and CYLD-deficient mice after DEN treatment (3, 6, 12, 24 and 48 h posttreatment). Representative blots of at least three separate experiments. Numbers above p-JNK1 blots represent a densitometric analysis of the protein bands; data were normalized to actin and are expressed as fold change relative to total JNK1. (**D**) The levels of p-JNK1 and total JNK1 in freshly isolated primary wild-type and CYLD-deficient hepatocytes after treatment with DEN for 24 h. Representative blots of at least two separate experiments. Numbers above p-JNK1 blot represent a densitometric analysis of the protein bands; data were normalized to actin and are expressed as fold change relative to total JNK1. (**E**) The levels of TRAF2 ubiquitination in livers of DEN-treated wild-type and CYLD-deficient mice (24 and 48 h posttreatment). Representative blots of at least two separate experiments. (**F**) The levels of c-MYC in livers from three different wild-type and two different CYLD-deficient mice after treatment with DEN for 48 h. (**G**) The levels of c-MYC in livers from non-treated wild-type and CYLD-deficient mice.

promoter activity in HCC cell lines (Figure 6D and Supplementary Figure 11C, available at *Carcinogenesis* Online). Furthermore, the c-MYC expression was significantly increased in tumors of *CYLD*$^{-/-}$ mice but not in tumors of wild-type mice (Figure 6E). Next, we analyzed whether inhibition of JNK is able to ameliorate proliferation and c-MYC expression in CYLD-deficient mice. Intraperitoneal injection of JNK-specific inhibitor SP600125 prior to DEN treatment significantly reduced cyclin D1 and c-MYC expression (Figure 6F), as well as the number of proliferating (Ki-67-positive) hepatocytes in CYLD-deficient mice (Figure 6G and H).

The results of the analyses of c-MYC protein expression in human HCC tissues (using TMA) are illustrated in Supplementary Table 3, available at *Carcinogenesis* Online. We observed nuclear c-MYC staining in 21 of 81 informative cases, whereas no c-MYC immunosignal was detectable in the remaining 57 HCC tissues. Representative immunohistochemical staining of c-MYC-positive and c-MYC-negative HCC tissues is depicted in Supplementary Figure 12, available at *Carcinogenesis* Online. Expression of c-MYC was significantly associated with a higher MiB-1 labeling index (Supplementary Table 3, available at *Carcinogenesis* Online). Furthermore, we observed a negative correlation between CYLD and c-MYC expression in human HCC (Supplementary Table 2, available at *Carcinogenesis* Online). These findings demonstrate that in conjunction, a reduced CYLD and a high c-MYC expression have a significant impact on the proliferation rate in human HCC cells and tissues.

Discussion

Hepatocarcinogenesis is a multistep process, characterized by accumulation and interplay of genetic alterations. In particular, mutations in proto-oncogenes and loss of tumor suppressor genes play a critical role in development and progression of human HCC (1–3). Cellular injury and release of growth factors and cytokines induce proliferation of hepatocytes, and a high hepatocyte proliferation rate is generally acknowledged as a predictive factor of human HCC development (27). Previous studies detected downregulation, or loss, of the *CYLD* gene in human HCC cell lines and tissues (17,28), and reduced copy numbers of the CYLD gene were observed in >30% of hepatitis C

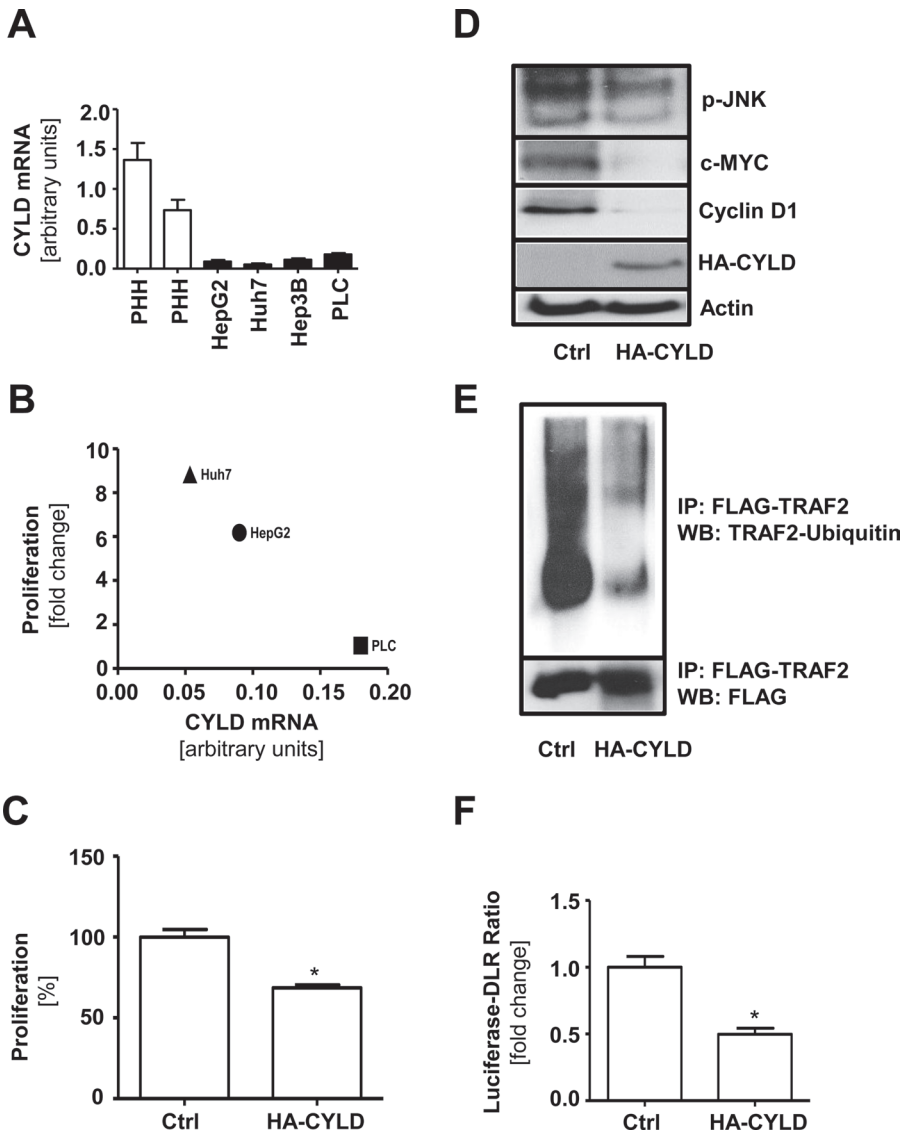

Fig. 5. Overexpression of CYLD in HCC cell lines prevents aberrant cell proliferation. (**A**) Expression levels of CYLD at the messenger RNA (mRNA) levels in primary hepatocytes from two donors, and the four HCC cell lines HepG2, Huh7, Hep3B and PLC. (**B**) Correlation between CYLD mRNA levels and proliferation rates of HCC cell lines (HepG2, Huh7 and PLC) after 72 h, using the 'Viability and cell count' protocol (NucleoCounter NC-3000; Chemometec). (**C**) Proliferation rate of HepG2 cells transiently transfected with control plasmid (Ctrl) or full-length CYLD expression plasmid, 72 h posttransfection, using the 'Viability and cell count' protocol (NucleoCounter NC-3000; Chemometec). Results are means ± SD of four separate experiments; $*P < 0.05$ denotes significant differences between the groups. (**D**) The expression levels of phospho-JNK1 (p-JNK1), c-MYC, HA-CYLD and cyclin D1 in HepG2 cells transfected with MOCK (Ctrl), or with human influenza hemagglutinin (HA)-tagged, full-length CYLD for 48 h. (**E**) TRAF2 ubiquitination in HepG2 cells, transiently transfected for 48 h with FLAG-TRAF2 and control plasmid (Ctrl), or with FLAG-TRAF2 and full-length CYLD. (**F**) AP-1 luciferase promoter activity in HepG2 cells transfected for 48 h with pGL2-AP1 and control plasmid (Ctrl), or with pGL2-AP1 and with full-length CYLD. The dual-luciferase reporter assay system was employed for the analysis (Promega). The promoter-driven Renilla control vector was used as an internal control to normalize the values of the experimental reporter gene. Results are means ± SD of four separate experiments; $*P < 0.05$ denotes significant differences between the groups.

virus-associated HCCs (29). The present study hypothesized that CYLD may act as a tumor suppressor in HCC, and liver cancer formation in mice lacking the *CYLD* gene was thus investigated.

CYLD-deficient animals, not developing spontaneous liver tumors up to the age of 1 year, were (as was shown in our experimental model) sensitive to induced HCC formation. Exposure of CYLD-deficient infant male mice to the chemical carcinogen DEN resulted in a significantly higher tumor incidence, and they developed significantly larger and more abundant tumors than their littermate controls. The increased tumor development in these mice was due to a dramatically elevated proliferation rate of the tumor cells, but tumor cell survival was not significantly altered. It has previously been suggested that CYLD deletion interferes with migration and invasion of tumor cells (30,31). In our model, we did not detect any invading or metastatic HCC cells in lymph nodes or in any other organs of CYLD-deficient animals (data not shown). Furthermore, overexpression of CYLD in HCC cells impaired proliferation but did not cause any significant changes in cell survival, adhesion or migration. Importantly, also in human HCC tissue, the CYLD expression showed an inverse correlation with mitotic activity but no correlation with tumor staging.

CYLD has previously been shown to interfere with different signaling pathways, including classical NF-κB, Bcl-3 and JNK, implicated in cell survival and proliferation (13–15). Although we did not observe any differences in NF-κB and Bcl-3 signaling, HCC isolated from CYLD-deficient mice contained elevated levels of activated JNK1. Already during the initiation phase of the DEN treatment or during the early phase of tumor development, a significant difference between $CYLD^{-/-}$ and $CYLD^{+/+}$ hepatocytes in terms of JNK1 activation was

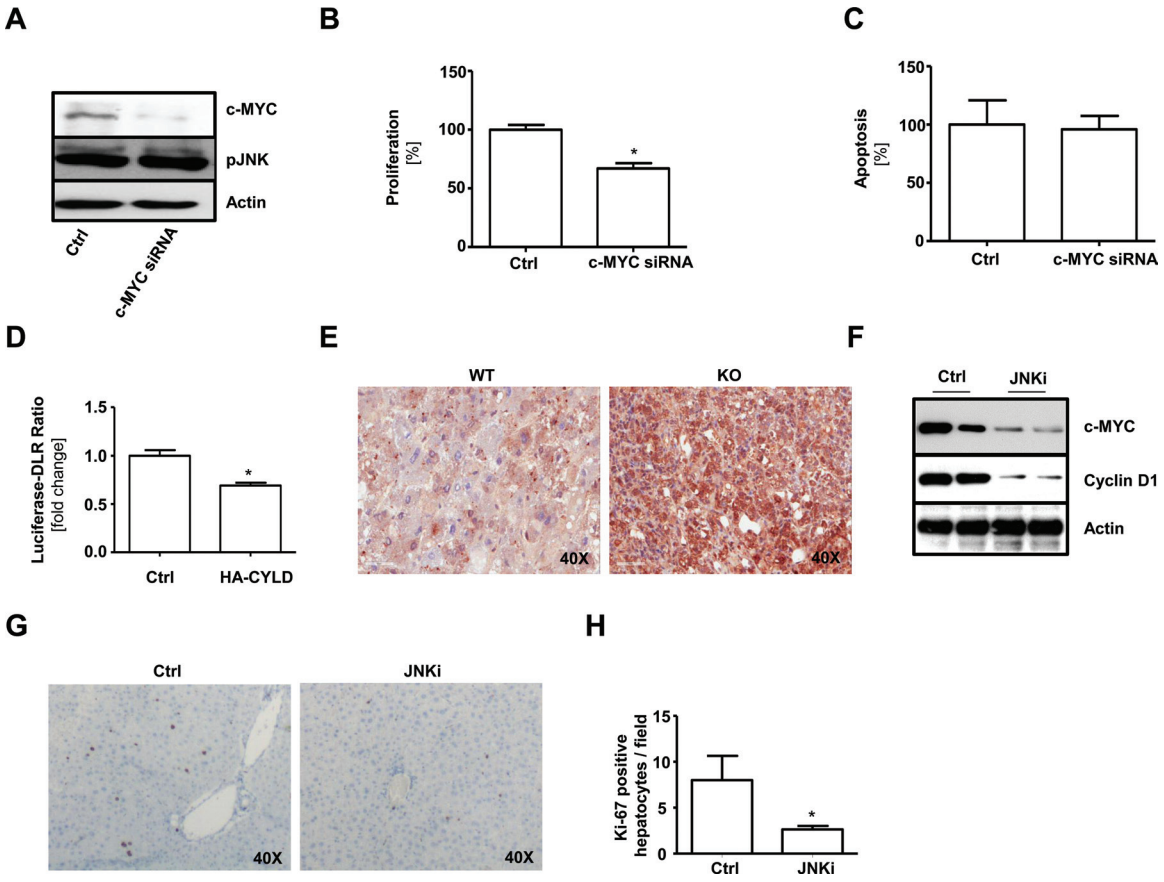

Fig. 6. Inverse correlation between CYLD and c-MYC protein expression in human liver tumor tissues. (**A**) Expression levels of c-MYC protein in HepG2 after transient transfection for 48 h with control (Ctrl) or c-MYC small interfering RNA (siRNA) oligos. (**B**) Evaluation of proliferation rate in HepG2 cells 48 h after being transiently transfected with control (Ctrl) or c-MYC siRNA oligos, using the 'Viability and cell count' protocol (NucleoCounter NC-3000; Chemometec). Results are means ± SD of three separate experiments; $*P < 0.05$ denotes significant differences between the groups. (**C**) DNA fragmentation assay results (NucleoCounter NC-3000 system) in HepG2 cells transiently transfected with control (Ctrl) or c-MYC siRNA oligos, 72 h posttransfection. Results are means ± SD of four separate experiments; $*P < 0.05$ denotes significant differences between the groups. (**D**) c-MYC luciferase promoter activity in HepG2 cells transfected for 48 h with c-MYC promoter luciferase and control plasmid (Ctrl), or with c-MYC promoter luciferase and full-length CYLD. The dual-luciferase reporter assay system was applied for the analysis (Promega). The promoter-driven Renilla control vector was used as an internal control to normalize the values of the experimental reporter gene. Results are means ± SD of three separate experiments; $*P < 0.05$ denotes significant differences between the groups. (**E**) Immunohistochemical analysis of c-MYC expression in 12 months old DEN-treated wild-type and CYLD-deficient animals. (**F**) The expression levels of cyclin D1 and c-MYC in livers from knockout (KO) mice treated with DEN ($n = 2$), or with the JNK-specific inhibitor (JNKi) SP600125 prior to DEN treatment ($n = 2$). (**G**) Immunohistochemical staining for Ki-67 and c-MYC in livers of KO mice treated with DEN, or with the JNKi SP600125 prior to DEN treatment. (**H**) Analysis of Ki-67-positive cells in livers of KO mice treated with DEN, or with the JNKi SP600125 prior to DEN treatment. Results are means ± SD; $*P < 0.05$ denotes significant differences between the groups.

evident. The immediate JNK1 signaling may affect cell proliferation and/or cell survival, associated with HCC (32–37). A previous study by Nikolaou *et al.* (18) reported that the expression of a deubiquitinase-deficient form of CYLD caused apoptosis of hepatocytes due to the activation of JNK. In contrast to their finding, a complete deletion of CYLD did (in the present study) not affect the number of apoptotic cells or the JNK1 activation under non-inducing conditions. Furthermore, we found that in mice, upon exposure to DEN, elevated JNK1 activation in *CYLD*$^{-/-}$ liver tissues promoted cell proliferation but did not alter the rate of cell survival. These phenotypic differences may be explained by CYLD deletion (of exon 9) being complete in our study, whereas only partial in the study by Nikolaou *et al.* (18).

JNK1-deficient mice have been described to be less susceptible to DEN-induced liver cancer, and human HCC sections have been shown to display an elevated activation of JNK1 in cancer cells, in comparison with adjacent non-cancerous tissue (38–40). In cancer cells, a sustained JNK1 phosphorylation through ubiquitination of TRAF2 may lead to transcriptional activation of target genes, and the AP-1 transcription factor is an important downstream signal of JNK activation (41).

Our study supports these findings; we observed that loss of CYLD did not result in deubiquitination of TRAF2. This facilitated activation of JNK1 and promoter activation of AP-1, leading to transcription of genes important for cell proliferation, such as cyclin D1 and c-MYC. These results suggest that inactivation of the JNK1-signaling pathway by CYLD reduces the c-MYC and cyclin D1 expressions, thus preventing aberrant proliferation of hepatocytes and tumor cells, which agrees with previous observations that JNK deletion results in a reduced expression of cyclin D1 in hepatocyte and HCC cell proliferation (39,42,43), and that cyclin D1 is an AP-1 target gene (44).

It has been shown earlier that JNK activation by external stimuli or growth factors leads to phosphorylation of AP-1 transcription factors, including c-Jun and Jun-D. The JNK docking motif of c-Jun are serine 63 and 73 leading to the activity of the kinase (45). In addition, a recent study demonstrated that JNK-dependent phosphorylation of c-Jun, releases c-Jun from the constitutively repressed complex containing histone deacetylases (46). JNK1 has also been shown to directly stabilize c-MYC protein levels by phosphorylation (47).

Our study actually uncovers a link between CYLD and c-MYC, *via* JNK1, offering a mechanistic insight into the role of CYLD deficiency in tumor initiation and progression. A small molecule c-MYC inhibitor has recently been shown to inhibit HCC cell growth and to sensitize these cells to chemotherapeutic agents (48). The identification

of the link between CYLD and c-MYC may be the foundation for exploring new therapeutic avenues for treating HCC, and potentially other kinds of tumors as well.

Supplementary material

Supplementary Tables 1–3 and Figures 1–12 can be found at http://carcin.oxfordjournals.org/

Funding

Swedish Society for Medical Research; the Swedish Cancer Foundation; the Swedish Medical Research Council; the Royal Physiographic Society in Lund; U-MAS Research Foundations; the European Research Council, under the European Union's Seventh Framework Programme for Research and Technology Development (260460 to R.M.); German Research Foundation (Deutche Forchungsgemeinschaft); the Medical Faculty of the University of Regensburg (ReForM-program), awarded to A.K.B. and C.H.

Acknowledgement

We thank Elise Nilsson and Rudolf Jung for excellent technical assistance.

Conflict of Interest Statement: None declared.

References

1. El-Serag,H.B. *et al.* (2008) Diagnosis and treatment of hepatocellular carcinoma. *Gastroenterology*, **134**, 1752–1763.
2. Farazi,P.A. *et al.* (2006) Hepatocellular carcinoma pathogenesis: from genes to environment. *Nat. Rev. Cancer*, **6**, 674–687.
3. Whittaker,S. *et al.* (2010) The role of signaling pathways in the development and treatment of hepatocellular carcinoma. *Oncogene*, **29**, 4989–5005.
4. Pickart,C.M. (2001) Mechanisms underlying ubiquitination. *Annu. Rev. Biochem.*, **70**, 503–533.
5. Weissman,A.M. (2001) Themes and variations on ubiquitylation. *Nat. Rev. Mol. Cell Biol.*, **2**, 169–178.
6. Nijman,S.M. *et al.* (2005) A genomic and functional inventory of deubiquitinating enzymes. *Cell*, **123**, 773–786.
7. Harhaj,E.W. *et al.* (2011) Deubiquitinases in the regulation of NF-κB signaling. *Cell Res.*, **21**, 22–39.
8. Deng,L.L. *et al.* (2012) Over-expressing CYLD augments antitumor activity of TRAIL by inhibiting the NF-κB survival signaling in lung cancer cells. *Neoplasma*, **59**, 18–29.
9. Massoumi,R. (2011) CYLD: a deubiquitination enzyme with multiple roles in cancer. *Future Oncol.*, **7**, 285–297.
10. Massoumi,R. *et al.* (2006) Cyld inhibits tumor cell proliferation by blocking Bcl-3-dependent NF-kappaB signaling. *Cell*, **125**, 665–677.
11. Massoumi,R. *et al.* (2009) Down-regulation of CYLD expression by Snail promotes tumor progression in malignant melanoma. *J. Exp. Med.*, **206**, 221–232.
12. Zhang,J. *et al.* (2006) Impaired regulation of NF-kappaB and increased susceptibility to colitis-associated tumorigenesis in CYLD-deficient mice. *J. Clin. Invest.*, **116**, 3042–3049.
13. Massoumi,R. (2010) Ubiquitin chain cleavage: CYLD at work. *Trends Biochem. Sci.*, **35**, 392–399.
14. Sun,S.C. (2008) Deubiquitylation and regulation of the immune response. *Nat. Rev. Immunol.*, **8**, 501–511.
15. Courtois,G. (2008) Tumor suppressor CYLD: negative regulation of NF-kappaB signaling and more. *Cell. Mol. Life Sci.*, **65**, 1123–1132.
16. Wickström,S.A. *et al.* (2010) CYLD negatively regulates cell-cycle progression by inactivating HDAC6 and increasing the levels of acetylated tubulin. *EMBO J.*, **29**, 131–144.
17. Hellerbrand,C. *et al.* (2007) Reduced expression of CYLD in human colon and hepatocellular carcinomas. *Carcinogenesis*, **28**, 21–27.
18. Nikolaou,K. *et al.* (2012) Inactivation of the deubiquitinase CYLD in hepatocytes causes apoptosis, inflammation, fibrosis, and cancer. *Cancer Cell*, **21**, 738–750.
19. Font-Burgada,J. *et al.* (2012) CYLD and HCC: when being too sensitive to your dirty neighbors results in self-destruction. *Cancer Cell*, **21**, 711–712.
20. Chu,L. *et al.* (2006) Adenoviral vector expressing CYLD augments antitumor activity of TRAIL by suppression of NF-kappaB survival signaling in hepatocellular carcinoma. *Cancer Biol. Ther.*, **5**, 615–622.
21. Urbanik,T. *et al.* (2011) Down-regulation of CYLD as a trigger for NF-κB activation and a mechanism of apoptotic resistance in hepatocellular carcinoma cells. *Int. J. Oncol.*, **38**, 121–131.
22. Gautheron,J. *et al.* (2012) A novel player in inflammation and cancer: the deubiquitinase CYLD controls HCC development. *J. Hepatol.*, **57**, 937–939.
23. Bosserhoff,A.K. *et al.* (2003) Specific expression and regulation of the new melanoma inhibitory activity-related gene MIA2 in hepatocytes. *J. Biol. Chem.*, **278**, 15225–15231.
24. Amann,T. *et al.* (2010) Reduced expression of fibroblast growth factor receptor 2IIIb in hepatocellular carcinoma induces a more aggressive growth. *Am. J. Pathol.*, **176**, 1433–1442.
25. Hellerbrand,C. *et al.* (2008) The novel gene MIA2 acts as a tumour suppressor in hepatocellular carcinoma. *Gut*, **57**, 243–251.
26. Sugino,T. *et al.* (2008) Sinusoidal tumor angiogenesis is a key component in hepatocellular carcinoma metastasis. *Clin. Exp. Metastasis*, **25**, 835–841.
27. Sangiovanni,A. *et al.* (2001) Hepatocyte proliferation and risk of hepatocellular carcinoma in cirrhotic patients. *Am. J. Gastroenterol.*, **96**, 1575–1580.
28. Aderca,I. *et al.* (2008) The JNK inhibitor SP600129 enhances apoptosis of HCC cells induced by the tumor suppressor WWOX. *J. Hepatol.*, **49**, 373–383.
29. Hashimoto,K. *et al.* (2004) Analysis of DNA copy number aberrations in hepatitis C virus-associated hepatocellular carcinomas by conventional CGH and array CGH. *Mod. Pathol.*, **17**, 617–622.
30. Gao,J. *et al.* (2008) The tumor suppressor CYLD regulates microtubule dynamics and plays a role in cell migration. *J. Biol. Chem.*, **283**, 8802–8809.
31. Miliani de Marval,P. *et al.* (2011) CYLD inhibits tumorigenesis and metastasis by blocking JNK/AP1 signaling at multiple levels. *Cancer Prev. Res. (Phila.)*, **4**, 851–859.
32. Min,L. *et al.* (2011) Mitogen-activated protein kinases in hepatocellular carcinoma development. *Semin. Cancer Biol.*, **21**, 10–20.
33. Papa,S. *et al.* (2009) Mechanisms of liver disease: cross-talk between the NF-kappaB and JNK pathways. *Biol. Chem.*, **390**, 965–976.
34. Wagner,E.F. *et al.* (2009) Signal integration by JNK and p38 MAPK pathways in cancer development. *Nat. Rev. Cancer*, **9**, 537–549.
35. Dhanasekaran,D.N. *et al.* (2008) JNK signaling in apoptosis. *Oncogene*, **27**, 6245–6251.
36. Weston,C.R. *et al.* (2007) The JNK signal transduction pathway. *Curr. Opin. Cell Biol.*, **19**, 142–149.
37. Johnson,G.L. *et al.* (2007) The c-jun kinase/stress-activated pathway: regulation, function and role in human disease. *Biochim. Biophys. Acta*, **1773**, 1341–1348.
38. Hui,L. *et al.* (2008) Proliferation of human HCC cells and chemically induced mouse liver cancers requires JNK1-dependent p21 downregulation. *J. Clin. Invest.*, **118**, 3943–3953.
39. Sakurai,T. *et al.* (2006) Loss of hepatic NF-kappa B activity enhances chemical hepatocarcinogenesis through sustained c-Jun N-terminal kinase 1 activation. *Proc. Natl Acad. Sci. USA*, **103**, 10544–10551.
40. Chang,Q. *et al.* (2009) Sustained JNK1 activation is associated with altered histone H3 methylations in human liver cancer. *J. Hepatol.*, **50**, 323–333.
41. Shaulian,E. (2010) AP-1–the Jun proteins: oncogenes or tumor suppressors in disguise? *Cell. Signal.*, **22**, 894–899.
42. Lu,X.P. *et al.* (1992) Induction of cyclin mRNA and cyclin-associated histone H1 kinase during liver regeneration. *J. Biol. Chem.*, **267**, 2841–2844.
43. Zhang,Y.J. *et al.* (1993) Amplification and overexpression of cyclin D1 in human hepatocellular carcinoma. *Biochem. Biophys. Res. Commun.*, **196**, 1010–1016.
44. Brooks,A.R. *et al.* (1996) Functional analysis of the human cyclin D2 and cyclin D3 promoters. *J. Biol. Chem.*, **271**, 9090–9099.
45. Kallunki,T. *et al.* (1996) c-Jun can recruit JNK to phosphorylate dimerization partners via specific docking interactions. *Cell*, **87**, 929–939.
46. Weiss,C. *et al.* (2003) JNK phosphorylation relieves HDAC3-dependent suppression of the transcriptional activity of c-Jun. *EMBO J.*, **22**, 3686–3695.
47. Noguchi,K. *et al.* (2001) ASK1-signaling promotes c-Myc protein stability during apoptosis. *Biochem. Biophys. Res. Commun.*, **281**, 1313–1320.
48. Lin,C.P. *et al.* (2007) Small-molecule c-Myc inhibitor, 10058-F4, inhibits proliferation, downregulates human telomerase reverse transcriptase and enhances chemosensitivity in human hepatocellular carcinoma cells. *Anticancer. Drugs*, **18**, 161–170.

Received May 14, 2013; revised August 29, 2013; accepted September 7, 2013